Reactivity of CHI3 with OH Radicals: X-Abstraction Reaction Pathways (X = H, I), Atmospheric Chemistry, and Nuclear Safety

ARTICLE *in* THE JOURNAL OF PHYSICAL CHEMISTRY A · SEPTEMBER 2014

Impact Factor: 2.69 · DOI: 10.1021/jp5051832 · Source: PubMed

3 AUTHORS:

Mária Sudolská
Palacký University of Olomouc
7 PUBLICATIONS **5** CITATIONS
SEE PROFILE

Florent Louis
Université des Sciences et Technologies de Lill…
45 PUBLICATIONS **401** CITATIONS
SEE PROFILE

Ivan Cernusak
Comenius University in Bratislava
77 PUBLICATIONS **752** CITATIONS
SEE PROFILE

THE JOURNAL OF PHYSICAL CHEMISTRY A

Article

pubs.acs.org/JPCA

Reactivity of CHI_3 with OH Radicals: X-Abstraction Reaction Pathways (X = H, I), Atmospheric Chemistry, and Nuclear Safety

Mária Sudolská,[†] Florent Louis,*[,‡] and Ivan Černušák*[,†]

[†]Department of Physical and Theoretical Chemistry, Faculty of Natural Sciences, Comenius University, Mlynská dolina CH1, 84215 Bratislava, Slovakia

[‡]PhysicoChimie des Processus de Combustion et de l'Atmosphère (PC2A), UMR 8522 CNRS/Lille1, Université Lille 1 Sciences et Technologies, Cité Scientifique, Bât. C11/C5, 59655 Villeneuve d'Ascq Cedex, France

Supporting Information

ABSTRACT: The X-abstraction (X = H, I) pathways in the reaction of CHI_3 with OH radical, a possible iodoform removal process relevant to the Earth's atmosphere and conditions prevailing in the case of a nuclear accident, have been studied applying highly correlated ab initio quantum chemistry methods and canonical transition-state theory to obtain reaction energy profiles and rate constants. Geometry optimizations of reactants, products, molecular complexes, and transition states determined at the MP2/cc-pVTZ level of theory have been followed by DK-CCSD(T)/ANO-RCC single-point energy calculations. Further improvement of electronic energies has been achieved by applying spin−orbit coupling, corrections toward full configuration interaction, vibration contributions, and tunneling corrections. Calculated reaction enthalpies at 0 K are −108.2 and −5.1 kJ mol^{-1} for the H- and I-abstraction pathways, respectively; the strongly exothermic H-abstraction pathway is energetically favored over the modestly exothermic I-abstraction one. The overall rate constant at 298 K based on our ab initio calculations is 4.90×10^{-11} cm^3 molecule^{-1} s^{-1}, with the I-abstraction pathway being the major channel over the temperature range of 250−2000 K. The CHI_3 atmospheric lifetime with respect to the removal reaction with OH radical is predicted to be about 6 h, very short compared to that of other halomethanes.

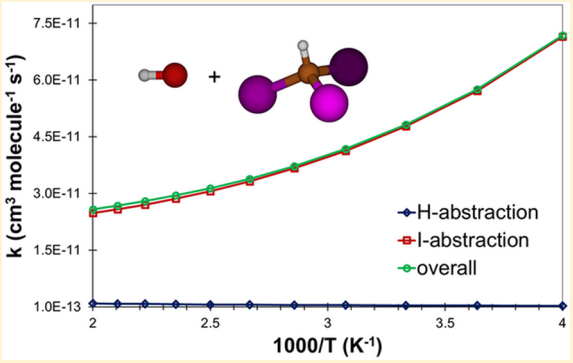

1. INTRODUCTION AND MOTIVATION

Mono- and polyhalogenated organic species, such as CH_3I, C_2H_5I, CH_2I_2, CH_2ICl, and CH_2IBr, are remarkable sources of atmospheric iodine, which plays a significant role in ozone destruction, causes shifts in the HO_x and NO_x ratios, resulting in the changed oxidation capacity of the atmosphere, and can also assist in the aerosol particle formation processes.[1−4] Beside the well-established role of organic iodides in the field of atmospheric chemistry, iodine organic compounds represent one of the volatile forms of radioiodine formed under the conditions during a serious accident of a nuclear reactor. As many of these compounds are difficult to be absorbed by postaccident filtration systems, they are still in the center of current research attention.[5−7] Radioiodine is one of the most important fission products that can be released from the reactor coolant system into the containment building and outer environment in the case of an accident. Short-lived isotope ^{131}I (half-life of 8 days) exists for a sufficiently long time after the release into the environment to pose danger to human health as a consequence of its biological activity (concentration in the human thyroid).[8]

Global organic halogenide release into the atmosphere is caused to the largest extent by micro- and macroalgae metabolism in the open oceans and sea coastal regions. The additional terrestrial sources of these organic compounds are, for example, rice paddies, wetlands, biomass burning, and terrestrial biomes.[4] When they reach the atmosphere, halogenated organic species are removed by photodissociation processes upon the formation of atomic halogens and can also react with species such as OH, Cl, and NO_3. In addition, they participate in heterogeneous reactions and reactions in the aqueous phase (e.g., in rain droplets, snow, and aerosol).[1−3]

In the coolant system and containment of a nuclear reactor, the presence of organic iodides results from the iodine release from fuel followed by the chemical and physical processes in gas and aqueous phases and on surfaces. In the gas phase, reactions of I_2 with organic compounds in the radiation field and with the participation of OH radicals are not as significant as those in the aqueous phase (as the consequence of substantially lower concentration of OH from water vapor radiolysis in the gas phase). Partitioning of volatile iodine organic species from water originating from the above-mentioned chemical reactions and organic iodine formation from gas or aqueous iodine with low molecular weight

Received: May 27, 2014
Revised: September 10, 2014
Published: September 10, 2014

   dx.doi.org/10.1021/jp5051832 | J. Phys. Chem. A 2014, 118, 9512−9520

hydrocarbons from paints on the surfaces are much more important sources of iodocarbons. Once iodocarbons are formed, they are prone to the destruction by β and γ radiation and reactions with reactive species resulting from water vapor and air radiolysis, for example, OH radicals and O atoms, analogously to the removal in the Earth's atmosphere.[5−7]

Iodoform (CHI_3) is not labeled as one of the pronounced iodine-substituted hydrocarbons released into the atmosphere (contrary to, e.g., CH_3I and CH_2I_2) nor is it among iodine organic compounds formed during a nuclear accident; to our knowledge, there are only a few experimental and theoretical works dealing with this species. So far, the presence of CHI_3 in the marine air resulting from algae and phytoplankton metabolic activities has been postulated by Carpenter et al.[9] and later confirmed by Urhahn and Ballschmiter,[10] and Martino et al.[11] and Urhahn and Ballschmiter[10] have recently identified this species in the marine air over the Atlantic Ocean utilizing high-resolution gas chromatography. In the latter work by Martino et al.,[11] it has been proposed that iodoform can be formed when seawater is exposed to ambient levels of ozone and dissolved iodine and organic matter are present at the same time. As for the case of a severe accident scenario, Holm et al.[12] suggested that CHI_3 could be formed after the radiolysis of methyl iodide.

Further studies on CHI_3 aimed to characterize its photodissociation, spectroscopic, and thermodynamic properties. Tu et al.[13] conducted spectroscopic measurements of four halogenated methanes including CHI_3 as photodissociation is one of the main paths of their removal in the troposphere. The authors have identified emission bands originating from the species such as CH, C_2, and atomic and molecular iodine; in addition, accurate anharmonicity parameters for I_2 have been obtained. The theoretical study performed by Marshall et al.[14] has been focused on a series of iodine-containing methanes including CHI_3. A correlated ab initio quantum chemistry approach was used to calculate geometry parameters, vibrational frequencies, and the enthalpies of formation of these species. As far as we know, the only measurement of the kinetics of the reaction involving CHI_3 and OH radicals, which are present both in the atmosphere and in the nuclear reactor during an accident, has been conducted by Zhang.[15] Here, a flash photolysis resonance fluorescence technique has been employed, and the overall reaction rate constant has been measured at 298 K, leading to the following value: $1.65 \pm 0.06 \times 10^{-11}$ cm^3 molecule^{-1} s^{-1}.

Despite extensive efforts carried out to understand the chemistry of organic iodides in the atmosphere and during a nuclear accident, there are still gaps in the overall and concise knowledge; the unresolved issues connected with phenomena such as fluxes of alkyl iodides from the oceans into the atmosphere, gas-phase photochemistry of reactive iodine species originating from organic iodine compounds, or the detailed characteristics of chemical and physical processes involving iodocarbons in the reactor coolant system and containment air request further investigation. As it follows from the short overview of publications dealing with CHI_3, additional research is needed to augment and confirm the present knowledge.

In this work, ab initio quantum chemistry methods and transition-state theory (TST) were used to determine the energetics and reaction rate coefficient for the reaction of CHI_3 with OH radicals. Two possible reaction pathways were taken into account, H-abstraction leading to the formation of CI_3 and H_2O and I-abstraction producing CHI_2 and HOI

$$CHI_3 + OH \rightarrow CI_3 + H_2O$$

$$CHI_3 + OH \rightarrow CHI_2 + HOI$$

The accurate determination of the reaction kinetic parameters is a challenging task—at least the chemical accuracy (± 4 kJ mol^{-1}) in energy evaluations is required. Therefore, the approach to obtaining the energies of molecules and molecular complexes has to employ all important corrections (basis set saturation, electron correlation, relativistic effects, spin-adaptation, vibration contributions, and tunneling corrections).

This article is the continuation of our previous studies on the kinetics of the reactions between hydroxyl radical and mono- and dihalogenated methanes, namely, CH_3I and CH_2I_2,[16] CH_2ICl,[17] and CH_2IBr,[18] aiming to acquire the reaction rate constants in partial fulfillment of the need to assess the significance of these species with respect to the reactions with hydroxyl radical. To the best of our knowledge, no temperature dependence of the reaction rate constant for CHI_3 with OH radicals has been reported in the literature.

2. COMPUTATIONAL METHODS

The optimized geometries of all stationary points on reaction profiles (reactants, products, molecular complexes, and TSs) were determined at the second-order Møller−Plesset perturbation theory (MP2)[19] as implemented in the Gaussian 03 program.[20] The Dunning's triple-ζ correlation-consistent basis sets cc-pVTZ were used for light atoms;[21] in the case of iodine, the Peterson's pseudopotential basis set of the same class[22] was employed to account for scalar relativistic effects in the optimization calculations. The intrinsic reaction coordinate (IRC) analyses[23,24] were performed at the same level of theory as geometry optimizations to confirm that the specific TS connects the different local minima (i.e., pre- and postreactive molecular complexes). For the OH radical, two electronic states with a 139.21 cm^{-1} splitting[25] in the $^2\Pi$ ground state were included in the calculation of the electronic partition function.

The calculated vibrational frequencies were scaled by an appropriate scaling factor (0.950)[26] to compensate for the errors arising from the anharmonic character of vibrational modes and the approximate electronic structure description. To improve the accuracy of the reaction rate calculations, the low-frequency vibrational modes corresponding to hindered (internal) rotations in the TS structures were treated by the 1D hindered rotor model as implemented in the code by Pfaendtner et al.[27,28] In this procedure, the vibrational modes were carefully inspected to identify possible internal rotations. Subsequent potential energy scans of the identified hindered rotations were obtained at the same level of theory as geometry optimizations, with the step size (dihedral angle) of 10°. These scans as well as the optimized geometries of the structures were finally used to calculate partition functions and thermodynamic properties. The harmonic approximation was adopted for all remaining vibrational modes.

We identified three low-frequency vibrational modes as hindered rotations in the H-abstraction TS structure, 20.0, 89.6, and 109.8 cm^{-1}. The first mode corresponds to the rotation of the H atom (in the OH subsystem) around the axis H···O (H in the CHI_3 subsystem, O in the OH subsystem); the other two modes are for the rotation of the OH top around the axis C−H (H in the CHI_3 subsystem). The rotational barriers (i.e.,

dx.doi.org/10.1021/jp5051832 | J. Phys. Chem. A 2014, 118, 9512−9520

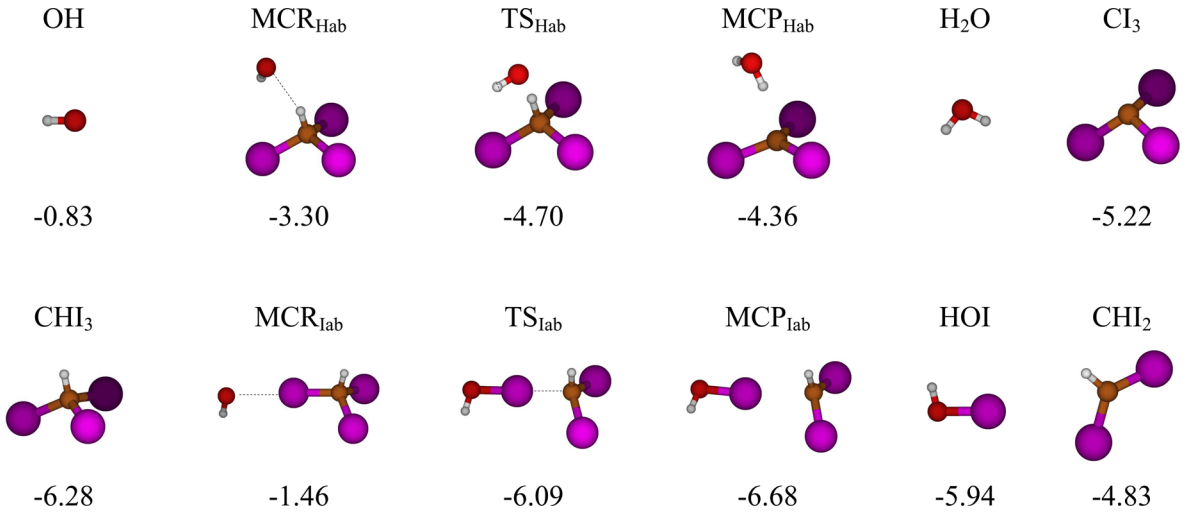

Figure 1. Molecular structures and SO corrections (kJ mol^{-1}) for the species in the reaction profiles. SO corrections for OH, HOI, and CHI_2 were taken from our previous papers.[17,18]

differences between electronic energies between the maximum and minimum at the potential curves) calculated at the MP2/cc-pVTZ level of theory were 3.1, 0.8, and 0.1 kJ mol^{-1}, respectively. In the case of the I-abstraction TS structure, two nearly degenerate vibrational modes (171.6 and 189.5 cm^{-1}) were treated as internal rotations of the H atom (in the HOI subsystem) around the axis I···O (the HOI subsystem) with the barrier of ∼5 kJ mol^{-1}. The scans of the potential energy surface as a function of the respective dihedral angle were performed as rigid scans, except for the third mode in the H-abstraction TS (partially relaxed scan). The calculated potential curves were not symmetrical (implying symmetry number 1 for all internal rotations).

In order to improve electronic energy predictions, the single-point energies at all optimized structures were evaluated at the coupled cluster theory including single, double, and non-iterative triple substitutions (CCSD(T)).[29] To account for scalar relativistic effects, which are inevitable in the calculations of heavy atoms like iodine,[30,31] the second-order Douglas–Kroll–Hess model[32−34] and the all-electron relativistic ANO-type basis sets on all atoms in the "large" contraction[35,36] were used: (8s4p3d1f)/[6s4p3d1f] for H, (14s9p4d3f2g)/[8s7p4d3f2g] for C and O, and (22s19p13d5f3g)/[10s9p8d5f3g] for I. The restricted open-shell Hartree–Fock reference wave function (ROHF) was used in the case of the open-shell species. A simple spin-adaptation scheme of the dominant DDVV part of T_2 excitation amplitudes with T_1 amplitudes nonadapted[37,38] was used to minimize the spin contamination resulting from the CCSD procedure. In the calculations of triples contribution to the CCSD energy, diagonal Fock matrix elements were used as denominators. This led to the one-component spin-adapted approach, DK-CCSD(T).

The CCSD(T) energies at all stationary points were further improved to account for the effects of higher excitations, that is, full configuration interaction (FCI) energies. The estimates of these effects were obtained by the continued-fraction (cf) correction; this extrapolation scheme was proposed by Goodson.[39] The method's performance is satisfactory even for stretched bonds in the molecular complexes and TSs. The cf correction can be applied when the convergence in CCSD is smooth.

Inclusion of the spin–orbit (SO) coupling is essential to obtain the accurate energy profiles of the reactions involving iodine-containing species.[17,18,40−42] In this work, the SO effects were calculated applying the state-averaged complete active space self-consistent field method, followed by the multistate second-order multiconfigurational perturbation theory and combined with the restricted active space state interaction method (SA-CASSCF/MS-CASPT2/RASSI-SO,[43] shortened as CASPT2/RASSI-SO). The active spaces in the CASSCF steps were chosen after some experimentation and careful analysis of the occupation numbers as well as the number of roots in SA-CASSCF and are as follows: CHI_3 (18e/14MO), CI_3 (17e/14MO), and all of the vdW complexes and both TSs (17e/14MO). We used the ANO-RCC-VQZP basis set in these calculations. The scalar relativistic effects within the CASPT2 method were incorporated using the second-order spin-free Douglas–Kroll–Hess Hamiltonian. In this manner, the SO effects represent an additional correction based on the one-electron SO Hamilton operator as an approximation to the SO coupling operator. For the coupled cluster energies and the SO corrections, we used the Molcas 7.8 suite.[32,44,45]

The results of SO calculations for both reaction pathways are collected in Figure 1. For the hydroxyl radical, the ground state ($^2\Pi$) splitting lowers the energy by −0.833 kJ mol^{-1}, and we can compare this number with the values determined by Huber[25] and Hess et al.[46] (−0.833 kJ mol^{-1}) and with the NIST-JANAF thermochemical database[47] (−0.836 kJ mol^{-1}). For the other reactants/products, complexes, and TSs, the resulting ground/excited states' SO coupling is almost quenched, primarily because of the large excitation energies. In these cases, the correction to the energy is the residual SO stabilization or simply second-order SO effect. To our knowledge, the SO coupling experimental data are not available for the stationary points collected in Figure 1; the only exception is the molecule HOI. Here, our calculated SO correction (−5.94 kJ mol^{-1}) is lower than the value estimated by Stevens et al.[48] (−1.69 kJ mol^{-1}). The differences arise from the different theoretical level applied and the selection of active space used (as already discussed in our previous study on CH_2IBr[18]).

The SO corrections between the prereactive complexes (MCR_{Hab} and MCR_{Iab}) and CHI_3 differ by ∼3 and ∼5 kJ

dx.doi.org/10.1021/jp5051832 | J. Phys. Chem. A 2014, 118, 9512−9520

mol^{-1}, respectively. The SO corrections are closer in the case of the postreactive complexes (MCP_{Hab} and MCP_{Iab}) and products (with the exception of H_2O); differences are below 2 kJ mol^{-1}. The Hammond's postulate[49] states that the TS geometry is reactant-like for exothermic reactions and it is product-like for endothermic reactions. In our previous papers focused on the abstraction reactions of CH_2ICl[17] and CH_2IBr,[18] SO splitting of the respective TS obeyed this rule, which was typical to the larger extent in the I-abstraction channels. The pertinent differences in SO splitting of reactants, TSs, and products were quite large, and these pathways were slightly endothermic (11.8 and 16.5 kJ mol^{-1} for CH_2ICl and CH_2IBr, respectively), the respective TS structures were product-like, and the SO corrections were comparable to the values for the products.[17,18] However, this is not exactly the case of the H- and I-abstractions from CHI_3 studied here. While the geometry of the I-abstraction TS (TS_{Iab}) resembles the geometry of the products (see Figure 1), the value of the SO correction (−6.09 kJ mol^{-1}) differs from both those of the reactant CHI_3 (−6.28 kJ mol^{-1}) and product HOI (−5.94 kJ mol^{-1}) by ∼0.2 kJ mol^{-1}. In the case of the H-abstraction, the TS structure is obviously reactant-like, as is expected for an exothermic reaction, but the SO correction (−4.70 kJ mol^{-1}) is closer to the value for the MCP structure (−4.36 kJ mol^{-1}) and CI_3 (−5.22 kJ mol^{-1}) rather than to the one obtained for CHI_3 (−6.28 kJ mol^{-1}).

Reaction rate constants have been calculated using the canonical TST.[50−57] The high-pressure limit rate constants, $k(T)$, were computed using the following expression

$$k(T) = \Gamma(T) \times \frac{k_B T}{h} \times \frac{Q_{TS}(T)}{Q_{OH}(T) Q_{CHI_3}(T)} \times \exp\left(-\frac{E_0}{k_B T}\right) \quad (1)$$

where $\Gamma(T)$ indicates the transmission coefficient used for the tunneling correction at temperature T and the terms $Q_{TS}(T)$, $Q_{OH}(T)$, and $Q_{CHI_3}(T)$ are the total partition functions for the TS and the reactants at the temperature T. In eq 1, the vibrationally adiabatic barrier height, E_0, is computed as the energy difference between the TS and the reactants, including zero-point energy corrections. k_B is Boltzmann's constant, and h is Planck's constant.

A similar approach was used for the calculation of the tunneling correction $\Gamma(T)$, as described in our previous works dealing with the reactions of OH with CH_2ICl[17] and CH_2IBr.[18] It corresponds to the widely used unsymmetrical one-dimensional Eckart function barrier.[58] This method works quite well for small or moderate tunneling corrections, which corresponds to our reaction. For the H-abstraction pathway, the calculated values range from 2.6 at 250 K to ∼1.0 at 2000 K, while there is no correction for the I-abstraction over the studied temperature range. It should be noticed however that more sophisticated and computationally demanding algorithms such as the ones developed by Truhlar[59−65] and Miller[66,67] should be used when tunneling corrections are much larger than those obtained in this work.

We have used the GPOP program[68] to extract the thermochemistry from Gaussian outputs as well as for the calculations of the Eckart tunneling corrections and the rate constants in the desired interval of temperatures.

3. RESULTS AND DISCUSSION

3.1. Geometries and Wavenumbers. The resulting MP2/cc-pVTZ geometry parameters and imaginary wavenumbers for molecular complexes and TSs for the H- and I-abstraction pathways are listed in Table 1. More detailed information regarding optimized geometries of the reactants and products, optimized Cartesian coordinates of the molecular complexes and TSs, wavenumbers of all stationary points, and literature enthalpies of formation at 298 K are presented in the Supporting Information, Tables S1−S7.

Table 1. Essential MP2/cc-pVTZ Geometry Parameters and Imaginary Wavenumbers for TSs and Molecular Complexes

H-abstraction	MCR_{Hab}	TS_{Hab}	MCP_{Hab}
r(C−H), Å	1.082	1.172	2.364
r(O−H), Å	2.397	1.340	0.962
θ(OHC), °	129.8	171.1	157.7
$\nu^{\#}$, cm^{-1}		1742i	
L^a		0.236	
I-abstraction	MCR_{Iab}	TS_{Iab}	MCP_{Iab}
r(C−I), Å	2.127	2.542	3.008
r(O−I), Å	3.154	1.987	1.993
θ (OIC), °	177.1	156.5	172.6
$\nu^{\#}$, cm^{-1}		210i	

[a]For the definition of the L parameter, see the text.

3.1.1. TSs. The H-abstraction pathway TS structure (TS_{Hab}) is characterized by a very small increase in the C−H bond length (1.172 Å compared to the equilibrium value of 1.082 Å in CHI_3) and a relatively long O−H bond length (1.340 versus 0.959 Å in the isolated H_2O molecule optimized at the same theoretical level). For the description of geometry changes of the TS, we used the L parameter defined as the ratio between the elongations of the bonds being broken and formed,[69] for example, for H-abstraction $L = \delta r(CH)/\delta r(OH)$, relative to its equilibrium value in the reactant/product. This value indicates the product- or reactant-like nature of the TS; a large value corresponds to the product-like structure, while a small value is typical for the reactant-like TSs. Our calculated value (0.236) is much smaller than 1 and is thus in agreement with the Hammond's postulate[49] predicting a reactant-like TS structure for an exothermic reaction.

In the I-abstraction pathway TS structure (TS_{Iab}), the C−I bond is stretched by quite a large amount (2.542 Å) from its equilibrium value in CHI_3 (2.129 Å). On the contrary, the O−I bond length is almost the same as that in HOI (the corresponding values are 1.987 and 1.992 Å, respectively). This leads to the conclusion that the TS structure has a product-like character.

In the TS_{Hab} and TS_{Iab} structures, the eigenvector associated with the imaginary wavenumber can be interpreted as a motion of the atom (H or I) that is transferred between carbon and oxygen atoms.

3.1.2. Molecular Complexes. To check both the reaction profiles, we performed the MP2/cc-pVTZ IRC calculations confirming that the weak van der Waals complexes (MCR's and MCP's) are connected with the specific TS structure.

For the H-abstraction pathway, the C−H bonds in the reactant complex HO···HCI_3 (MCR_{Hab}) and in the CHI_3 are the same (1.082 Å). The O−H bond being formed in the

dx.doi.org/10.1021/jp5051832 | J. Phys. Chem. A 2014, 118, 9512−9520

reaction process is much longer in MCR_{Hab} (2.397 Å) compared to that in TS_{Hab} (1.340 Å).

On the contrary, the breaking C−H bond in the product complex HOH···CI_3 (MCP_{Hab}) is much longer (2.364 Å) than that in the respective TS structure. The length of the new O−H bond in MCP_{Hab} (0.962 Å) is approaching the equilibrium value in H_2O (0.959 Å).

In the I-abstraction pathway, the reactant complex HO···$ICHI_2$ (MCR_{Iab}) is formed via oxygen atom approach to CHI_3. Upon moving toward TS_{Iab} and the product complex HOI···CHI_2 (MCP_{Iab}), the breaking bond C−I lengthens from 2.127 Å (nearly the same length as in CHI_3, 2.129 Å) to 2.542 and 3.008 Å, respectively. The initial intermolecular bond O−I in MCR_{Iab} (3.154 Å) shortens substantially in TS_{Iab} (1.987 Å) and MCP_{Iab} (1.993 Å), approaching its equilibrium value in HOI (1.992 Å).

3.2. Energetics. The CCSD(T) electronic binding energies together with the contributions of the SO, cf, and zero-point vibrational energy (ZPE) corrections for the molecular complexes, TSs (i.e., activation barriers), and overall reaction energies for H- and I-abstraction pathways are collected in Tables 2 and 3, respectively. Final energy profiles (electronic energy differences ΔE, and enthalpies ΔH at 0 and 298 K) of both reaction channels are in Figure 2.

Table 2. H-Abstraction Pathway Summary of the Energy Contributions to Enthalpies at 0 K (in kJ mol^{-1}) at the CCSD(T)/ANO-RCC-Large//MP2/cc-pVTZ[a] Level of Theory along with SO Corrections Calculated at the CASPT2/RASSI/ANO-RCC-VQZP Level of Theory

H-abstraction pathway	forward		reverse		equilibrium
reaction step	OH + CHI_3 → MCR_{Hab}	OH + CHI_3 → TS_{Hab}	H_2O + CI_3 → MCP_{Hab}	H_2O + CI_3 → TS_{Hab}	OH + CHI_3 = H_2O + CI_3
	ΔH_{0K}	$\Delta H^{\ddagger}_{0K}$	ΔH_{0K}	$\Delta H^{\ddagger}_{0K}$	$\Delta_r H_{0K}$
CCSD(T)	−14.86	9.08	−8.99	119.67	−110.59
ZPE correction	2.77	−8.22	2.93	−10.07	1.85
SO correction	3.82	2.42	0.85	0.52	1.90
cf correction	1.81	0.96	2.69	2.33	−1.38
$CCSD(T)_{total}$	−6.45	4.24	−2.52	112.45	−108.22[b]

[a]For iodine, we used cc-pVTZ-PP basis in MP2 optimizations. [b]$\Delta_r H_{298K}$ = −107.45 kJ mol^{-1}.

The ZPE correction destabilizes the molecular complexes in both the H- and I-abstraction pathways; these destabilizing contributions range from 2.15 (MCR_{Iab}) to 3.67 kJ mol^{-1} (MCP_{Iab}). This is also the case of the I-abstraction TS, but the ZPE contributions (7.80 and 5.47 kJ mol^{-1} for the forward and reverse directions, respectively) are higher than the chemical accuracy threshold (±4 kJ mol^{-1}). On the contrary, the stability of the TS with respect to the reactants and products in the H-abstraction pathway is higher when the ZPE contribution (−8.22 and −10.07 kJ mol^{-1} for the forward and reverse directions, respectively) is included (see also Figure 2a,b).

The destabilization of the molecular complexes and TSs due to the SO effects is more pronounced in the I-abstraction pathway, 5.65 kJ mol^{-1} for MCR_{Iab} (forward direction) and 5.20 kJ mol^{-1} for MCP_{Iab} and 5.79 kJ mol^{-1} for TS_{Iab} (reverse direction), compared to the H-abstraction counterparts with the SO correction contributions in the range of 0.52−3.82 kJ mol^{-1}. The cf correction has generally a destabilizing effect and

Table 3. I-Abstraction Pathway Summary of the Energy Contributions to Enthalpies at 0 K (in kJ mol^{-1}) at the CCSD(T)/ANO-RCC-Large//MP2/cc-pVTZ[a] Level of Theory along with SO Corrections Calculated at the CASPT2/RASSI/ANO-RCC-VQZP Level of Theory[b]

I-abstraction pathway	forward		reverse		equilibrium
reaction step	OH + CHI_3 → MCR_{Iab}	OH + CHI_3 → TS_{Iab}	HOI + CHI_2 → MCP_{Iab}	HOI + CHI_2 → TS_{Iab}	OH + CHI_3 = HOI + CHI_2
	ΔH_{0K}	$\Delta H^{\ddagger}_{0K}$	ΔH_{0K}	$\Delta H^{\ddagger}_{0K}$	$\Delta_r H_{0K}$
CCSD(T)	−10.54	−18.62	−21.91	−13.02	−5.60
ZPE correction	2.15	7.80	3.67	5.47	2.34
SO correction	5.65	1.02	5.20	5.79	−3.65
cf correction	1.87	0.69	−0.48	−1.12	1.81
$CCSD(T)_{total}$	−0.86	−9.10	−13.51	−2.89	−5.10[c]

[a]For iodine we used cc-pVTZ-PP basis in MP2 optimizations. [b]Energies of the reactants are set to 0 kJ mol^{-1}. [c]$\Delta_r H_{298K}$ = −7.45 kJ mol^{-1}.

ranges from 0.69 kJ mol^{-1} (TS_{Iab}, forward direction) to 2.69 kJ mol^{-1} (MCP_{Hab}, reverse direction). The only exceptions are the reverse MCP_{Iab} and TS_{Iab} with the slightly negative cf contributions (−0.48 and −1.12 kJ mol^{-1}, respectively).

There is a significant contribution of the activation entropy in both reaction channels (from −100 to −120 J mol^{-1} K^{-1}) leading to positive values of $\Delta G^{\neq}_{298K}$.The resulting activation Gibbs energies are +32.3 kJ mol^{-1} for H-abstraction and +22.8 kJ mol^{-1} for I-abstraction. These were used in the rate constants calculation.

The basis set superposition error (BSSE) correction has not been included, but this contribution to the overall energy differences at the applied level of theory has been previously estimated to be within the chemical accuracy threshold.[16−18] Although it is important to account for all known possible sources of errors to minimize the cumulative effect of missing corrections, we do not present the counterpoise correction contribution due to the high computational demands of the CCSD(T)/ANO-RCC-Large calculations of the species containing three iodine atoms and the BSSE unambiguous determination in the case of the forward and reverse reaction barriers.

The exothermicity of both abstraction pathways is slightly altered when the ZPE, SO, and cf corrections are included (2.37 and 0.50 kJ mol^{-1} for H- and I-abstraction, respectively). In the case of H-abstraction, the final reaction enthalpy (at 0 K) is −108.22 kJ mol^{-1}. Iodine abstraction is moderately exothermic with an overall reaction enthalpy of −5.10 kJ mol^{-1}, which can be explained in the terms of C−H and C−I bond energy differences (431 and 239 kJ mol^{-1}, respectively).

In the series of iodomethanes CH_3I, CH_2I_2, and CHI_3, the exothermicity of H-abstraction increases, and the corresponding reaction enthalpies at 0 K are shifted toward more negative values (−78.7, −90.1, and −108.2 kJ mol^{-1} for CH_3I, CH_2I_2,[16] and CHI_3 (this work), respectively. The endothermicity of I-abstraction from CH_3I and CH_2I_2 (31.4 and 14.3 kJ mol^{-1}, respectively) changes into the modest exothermicity in the case of CHI_3 (−5.1 kJ mol^{-1}). These trends could be attributed to the different polarization and strength of the C−H and C−I bonds in iodomethanes due to the electron density withdrawing effect of iodine atoms.

dx.doi.org/10.1021/jp5051832 | J. Phys. Chem. A 2014, 118, 9512−9520

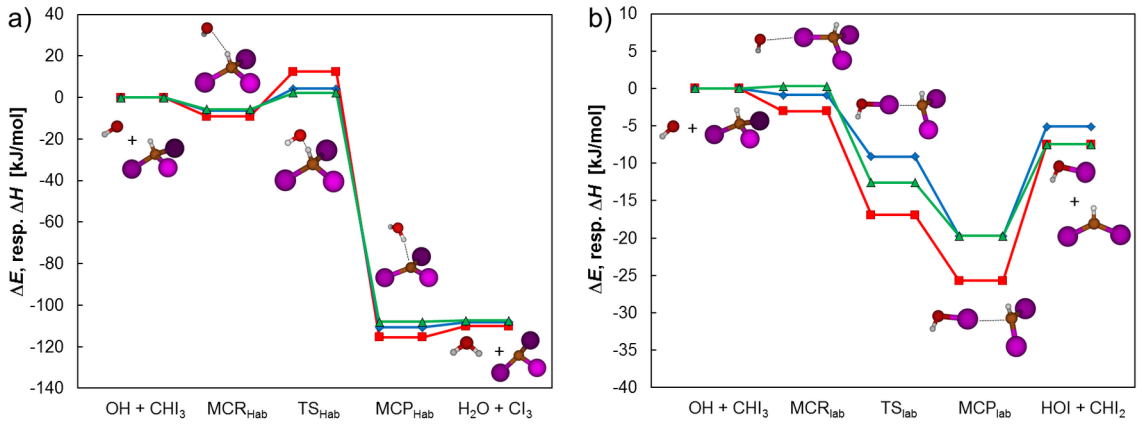

Figure 2. Energy profiles for the H- and I-abstraction pathways (in kJ mol^{-1}): ΔE (squares), ΔH_{0K} (diamonds), and ΔH_{298K} (triangles) for (a) H-abstraction and (b) I-abstraction pathways. Level of theory: CCSD(T)/ANO-RCC-Large//MP2/cc-pVTZ (cc-pVTZ-PP for iodine), including cp, cf and SO corrections. Activation Gibbs free energies: 32.3 kJ mol^{-1} (H-abstraction) and 22.8 kJ mol^{-1} (I-abstraction). Energies of the reactants are set to 0 kJ mol^{-1}.

Table 4. Summary of the Rate Constants Evaluated for Six Temperatures at the CCSD(T)/ANO-RCC-Large//MP2/cc-pVTZ[a] Level (cm^3 molecule^{-1} s^{-1}) with Hindered Rotor Corrections Included

	Rate Constant temperature (K)					
	250	300	500	800	1000	2000
H-abstraction	3.90×10^{-13}	4.90×10^{-13}	1.04×10^{-12}	1.99×10^{-12}	2.77×10^{-12}	8.72×10^{-12}
I-abstraction	7.16×10^{-11}	4.79×10^{-11}	2.49×10^{-11}	2.16×10^{-11}	2.25×10^{-11}	3.48×10^{-11}
overall	7.20×10^{-11}	4.84×10^{-11}	2.60×10^{-11}	2.36×10^{-11}	2.53×10^{-11}	4.35×10^{-11}

[a]For iodine, we used cc-pVTZ-PP basis in MP2 optimizations.

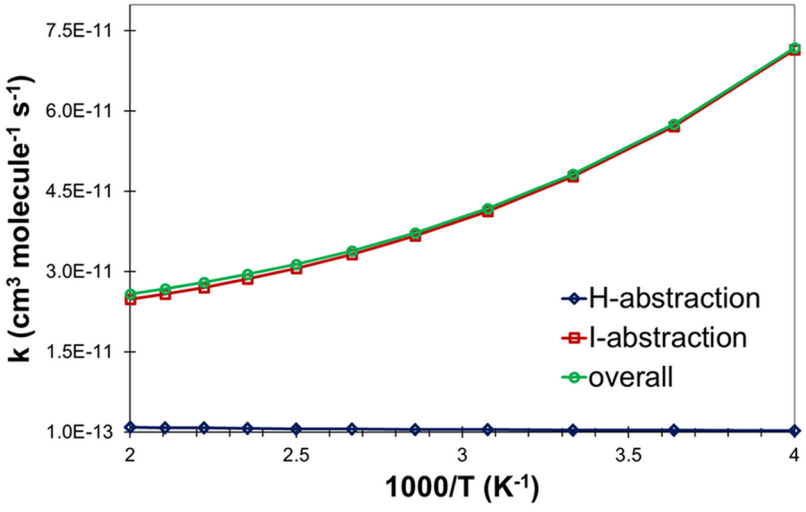

Figure 3. Temperature dependence of the rate constants for the H-abstraction (diamonds) and I-abstraction (squares) and the overall rate constant (circles).

The reaction enthalpies at 298 K ($\Delta_r H°_{298K}$) for both pathways have also been calculated considering the particular species heats of formation ($\Delta_f H°_{298K}$) taken from the literature (Supporting Information, Table S7). To our knowledge, there are three literature values available for CHI_3; the most recent one calculated at the QCISD(T)/6-311+G(3df,2p)//QCISD/6-311G(d,p) level of theory by Marshall et al.[14] (208.5 ± 9.9 kJ mol^{-1}) is in a good agreement with the value evaluated by Kudchadker and Kudchadker[70,71] (210.9 ± 4.2 kJ mol^{-1}). However, the last value of the heat of formation determined on the basis of combustion calorimetry experiments performed by Carson et al.[72] differs from these values substantially (251.0 ± 1.4 kJ mol^{-1}). The standard enthalpies of formation at 298 K for radicals CI_3 and CHI_2 have been determined by Marshall et al.,[14] Seetula,[73] and Louis et al.,[16] employing ab initio methods.

Here, the literature values of $\Delta_f H°_{298K}$ (all in kJ mol^{-1}) from Kudchadker and Kudchadker[70,71] (CHI_3, 210.9 ± 4.2), Marshall et al.[14] (CI_3, 369.1 ± 9.9), Louis et al.[16] (CHI_2, 298.3), Chase[47] (OH, 39.0 ± 1.2; H_2O, −241.8), and Šulková et al.[74] (HOI, −69.0 ± 3.7) were taken (see also Supporting Information Table S7). Reaction enthalpies calculated from these literature data are for the H-abstraction pathway, −122.6

dx.doi.org/10.1021/jp5051832 | J. Phys. Chem. A 2014, 118, 9512−9520

± 15.4 kJ mol^{-1}, and for the I-abstraction pathway, −20.6 ± 9.1 kJ mol^{-1}. Our calculated reaction enthalpy at 298 K for the H-abstraction pathway (−107.5 kJ mol^{-1}) is nearly at the upper bound of the $\Delta_r H^\circ_{298K}$ obtained from the respective literature data. However, in the case of the I-abstraction pathway, the reaction enthalpy determined on the basis of our ab initio calculations (−7.5 kJ mol^{-1}) differs at least by ∼4 kJ mol^{-1} from the upper bound of its literature counterpart if we take in account the pertinent uncertainties.

3.3. Rate Constants. The temperature dependence of rate constants has been calculated at the CCSD(T)/ANO-RCC-Large//MP2/cc-pVTZ level of theory including three corrections to the potential energies (ZPE, SO, and extrapolation to full CI) for both pathways. In Table 4, we have summarized the computed values at six different temperatures with the hindered rotor corrections included. The temperature dependence of the rate constants is displayed in Figure 3 for both reaction channels and also the overall reaction rate.

The I-abstraction pathway is the major channel over the whole temperature range of interest. The highest contribution of the H-abstraction pathway to the overall constant is observed at 2000 K, where it reaches about 20%. The opposite trend was observed in the case of the reactions of OH radicals with CH_2ICl[17] and CH_2IBr,[18] where the major channel was the H-abstraction.

The modified three-parameter Arrhenius expression $k(T) = B \times T^n \exp(-E_a/RT)$ fitted to the overall rate constant computed in the range 250−2000 K is

$$k\ (\text{in cm}^3\ \text{molecule}^{-1}\ \text{s}^{-1}) = 2.25 \times 10^{-16} T^{1.53} \exp\left(\frac{1065}{T}\right)$$

Using the above expression, one can derive k(277 K) = 5.74 × 10^{-11} cm^3 molecule^{-1} s^{-1} and k(298 K) = 4.90 × 10^{-11} cm^3 molecule^{-1} s^{-1}. Our calculated value at 298 K is in fair agreement with its experimental counterpart as measured by Zhang (1.65 × 10^{-11} cm^3 molecule^{-1} s^{-1}) using the flash photolysis/resonance fluorescence setup.[15]

3.4. Estimate of the Atmospheric Lifetime. Hydroxyl radical represents the main tropospheric species for the removal reactions of hydrogen-containing compounds. Using the recipe of Prather and Spivakovsky[75] and the procedure detailed in our previous publications,[17,18] we can estimate the atmospheric lifetime of CHI_3 to be about 6 h. No data are present in the literature concerning the rates of other removal processes such as photolysis or gas-phase reactions with chlorine atoms. Undoubtedly, the atmospheric lifetime of CHI_3 is very short by comparison to all other halomethanes.[17,18,76]

4. CONCLUSIONS

The atmospheric chemical reactivity of CHI_3 toward OH has been studied employing high-level ab initio methods. The optimized geometries of stationary points at H- and I-abstraction energy profiles (reactants, products, TSs, and pre- and postreactive molecular complexes) were obtained at the MP2/cc-pVTZ level of theory. The final electronic energies of these optimized structures and reaction enthalpies for both abstraction channels were determined utilizing the DK-CCSD(T)/ANO-RCC-Large approach involving scalar relativistic effects and high electron correlation and adding energy contributions arising from SO coupling, correction to the FCI limit, and scaled vibrational corrections. Calculated ab initio energies were used in the determination of rate constants and estimation of the atmospheric lifetime of CHI_3 with respect to the OH radical reaction.

On the basis of our calculations, the following can be concluded:

(1) The H-abstraction pathway is strongly exothermic ($\Delta_r H_{0K}$ = −108.2 kJ mol^{-1}), in contrast to the I-abstraction pathway, which is slightly exothermic ($\Delta_r H_{0K}$ = −5.1 kJ mol^{-1}), which is in accordance with the differences in the C−H and C−I bond strengths (431 compared to 239 kJ mol^{-1}).[77]

(2) The overall rate constant at 298 K is 4.90 × 10^{-11} cm^3 molecule^{-1} s^{-1}. In the temperature range of interest (from 250 to 2000 K), the I-abstraction channel prevails over the H-abstraction one. The contribution of the H-abstraction channel increases with the increasing temperature and reaches ∼20% at 2000 K. These results suggest that the H-abstraction pathway is more significant under the temperatures prevailing in the reactor coolant system and containment building of a nuclear reactor during an accident compared to the Earth's atmosphere. Consequently, the role of CHI_3 should be reconsidered in the nuclear accident simulations. On the contrary, the H-abstraction channel is the major one in the case of the previously studied halomethanes.[17,18]

(3) The estimated atmospheric lifetime of CHI_3 affected by the reaction with OH is about 6 h, which is very short compared to other halogen-substituted methanes.[17,18,76]

(4) Compared to the rate constants at room temperature for the reactions of CHI_3 and CH_3I with OH radical (4.9 × 10^{-11} cm^3 molecule^{-1} s^{-1} for CHI_3 and (0.6−1.2) × 10^{-13} cm^3 molecule^{-1} s^{-1} for CH_3I[78−81]), one may conclude that iodoform could have a more significant role in the iodine chemistry considering the OH reaction than methyl iodide, which has been often taken as a representative of organic iodides in nuclear research. Our results thus agree with the assumption that other iodocarbons should be also taken into account and support the postulate of Carpenter et al.[9] that short-lived iodocarbons such as $CHIBr_2$, CHI_2Br, and CHI_3 may also play an important role in coastal atmospheric iodine chemistry.

■ ASSOCIATED CONTENT

Supporting Information

MP2/cc-pVTZ-optimized geometries for the reactants and products, transition states, and molecular complexes (Tables S1 and S2), unscaled MP2/cc-pVTZ harmonic vibrational frequencies (Tables S3−S6), and standard enthalpy of formation at 298 K taken from the literature (Table S7). This material is available free of charge via the Internet at http://pubs.acs.org.

■ AUTHOR INFORMATION

Corresponding Authors

*E-mail: cernusak@fns.uniba.sk. Phone: +4212 6029 6429 (I.Č.).

*E-mail: florent.louis@univ-lille1.fr. Phone: +3332 033 6332 (F.L.).

Author Contributions

The manuscript was written through contributions of all authors. All authors have given approval to the final version of the manuscript.

Notes

The authors declare no competing financial interest.

■ ACKNOWLEDGMENTS

Computer time for part of the theoretical calculations was kindly provided by the Centre de Ressources Informatiques de Haute Normandie (CRIHAN) and the Centre de Ressources Informatiques (CRI) of the University of Lille1. We appreciate the support from the French ANR agency under Contract No. ANR-11-LABX-0005 "Chemical and Physical Properties of the Atmosphere" (CaPPA) and Slovak Grant Agencies APVV (Grant APVV-0059-10) and VEGA (Grant 1/0092/14). This work was supported also by the Research & Development Operational Program funded by the ERDF: Amplification of the Centre of Excellence on Green Chemistry Methods and Processes (CEGreen-II 26240120025).

■ REFERENCES

(1) Finlayson-Pitts, B. J.; Pitts, J. N., Jr. *Chemistry of the Upper and Lower Atmosphere. Theory, Experiments, and Applications*; Academic Press: San Diego, CA, 2000.

(2) von Glasow, R.; Crutzen, P. J. Tropospheric Halogen Chemistry. In *The Atmosphere*; Keeling, R. F., Ed; Elsevier−Pergamon: Oxford, U.K., 2006; Vol. *4*, pp 21−64.

(3) Holloway, A. M.; Wayne, R. P. *Atmospheric Chemistry*; Royal Society of Chemistry: Cambridge, U.K., 2010.

(4) Saiz-Lopez, A.; Plane, J. M. C.; Baker, A. R.; Carpenter, L. J.; von Glasow, R.; Gómez Martín, J. C.; McFiggans, G.; Saunders, R. W. Atmospheric Chemistry of Iodine. *Chem. Rev.* **2011**, *112*, 1773−1804.

(5) *Insights into the Control of the Release of Iodine, Cesium, Strontium and other Fission Products in the Containment by Severe Accident Management, NEA/CSNI/R(2000)9*; Nuclear Energy Agency: Issy-les-Moulineaux, France, 2009.

(6) Clément, B.; Cantrel, L.; Ducros, G.; Funke, F.; Herranz, L.; Rydl, A.; Weber, G.; Wren, C. *State of the Art Report on Iodine Chemistry, NEA/CSNI/R(2007)1*; Nuclear Energy Agency: Issy-les-Moulineaux, France, 2007.

(7) Glowa, G. A.; Moore, C. C. J. *Behaviour of Iodine Project. Final Summary Report. NEA/CSNI/R(2011)11*; Nuclear Energy Agency: Issy-les-Moulineaux, France, 2011.

(8) Zilliacus, R.; Koukkar, P.; Karjunen, T.; Sjövall, H. *Formation and Behaviour of Organic Iodine. NKS-42*; Nordic Nuclear Safety Research: Roskilde, Denmark, 2002.

(9) Carpenter, L. J.; Sturges, W. T.; Penkett, S. A.; Liss, P. S.; Alicke, B.; Hebestreit, K.; Platt, U. Short-Lived Alkyl Iodides and Bromides at Mace Head, Ireland: Links to Biogenic Sources and Halogen Oxide Production. *J. Geophys. Res.: Atmos.* **1999**, *104*, 1679−1689.

(10) Urhahn, T.; Ballschmiter, K. Analysis of Halogenated C1/C2-Trace Compounds in Marine Atmosphere. *Fresenius' J. Anal. Chem.* **2000**, *366*, 365−367.

(11) Martino, M.; Mills, G. P.; Woeltjen, J.; Liss, P. S. A New Source of Volatile Organoiodine Compounds in Surface Seawater. *Geophys. Res. Lett.* **2009**, *36*, L01609.

(12) Holm, J.; Kärkelä, T.; Auvinen, A.; Glänneskog, H.; Ekberg, C. *Experimental Study on Iodine Chemistry (EXSI). Containment Experiments with Methyl Iodide. NKS-245*; Nordic Nuclear Safety Research: Roskilde, Denmark, 2011.

(13) Tu, C.-P.; Cheng, H.-I.; Chang, B.-C. Spectroscopic Study of the I_2 Formation from the Photolysis of Iodomethanes (CHI_3, CH_2I_2, CH_3I, and CH_2ICl) at Different Wavelengths. *J. Phys. Chem. A* **2013**, *117*, 13572−13577.

(14) Marshall, P.; Srinivas, G. N.; Schwartz, M. A Computational Study of the Thermochemistry of Bromine- and Iodine-Containing Methanes and Methyl Radicals. *J. Phys. Chem. A* **2005**, *109*, 6371−6379.

(15) Zhang, S. *Etudes cinétiques de l'oxydation radicalaire en phase gazeuse d'iodures organiques et de la formation de particules d'oxydes d'iode sous conditions simulées de l'enceinte d'un réacteur nucléaire en situation d'accident grave*. Ph.D. Thesis, Aix-Marseille Université, Marseille Cedex, France, June 2012.

(16) Louis, F.; Černušák, I.; Canneaux, S.; Mečiarová, K. Atmospheric Reactivity of CH_3I and CH_2I_2 with OH Radicals: A Comparative Study of the H- versus I-Abstraction. *Comput. Theor. Chem.* **2011**, *965*, 275−284.

(17) Šulková, K.; Šulka, M.; Louis, F.; Neogrády, P. Atmospheric Reactivity of CH_2ICl with OH Radicals: High-Level OVOS CCSD(T) Calculations for the X-Abstraction Pathways (X = H, Cl, or I). *J. Phys. Chem. A* **2013**, *117*, 771−782.

(18) Šulka, M.; Šulková, K.; Louis, F.; Neogrády, P.; Černušák, I. A Theoretical Study of the X-Abstraction Reactions (X = H, Br, or I) from CH_2IBr by OH Radicals: Implications for Atmospheric Chemistry. *Z. Phys. Chem.* **2013**, *227*, 1337−1359.

(19) Møller, C.; Plesset, M. S. Note on an Approximation Treatment for Many-Electron Systems. *Phys. Rev.* **1934**, *46*, 618−622.

(20) Frisch, M. J.; Trucks, G. W.; Schlegel, H. B.; Scuseria, G. E.; Robb, M. A.; Cheeseman, J. R.; Montgomery, J. A., Jr.; Vreven, T.; Kudin, K. N.; Burant, J. C.; et al. *Gaussian 03*, revision D.01; Gaussian, Inc.: Wallingford, CT, 2004.

(21) Dunning, T. H., Jr. Gaussian Basis Sets for Use in Correlated Molecular Calculations. I. The Atoms Boron through Neon and Hydrogen. *J. Chem. Phys.* **1989**, *90*, 1007−1023.

(22) Peterson, K. A.; Shepler, B. C.; Figgen, D.; Stoll, H. On the Spectroscopic and Thermochemical Properties of ClO, BrO, IO, and Their Anions. *J. Phys. Chem. A* **2006**, *110*, 13877−13883.

(23) Gonzalez, C.; Schlegel, H. B. An Improved Algorithm for Reaction Path Following. *J. Chem. Phys.* **1989**, *90*, 2154−2161.

(24) Gonzalez, C.; Schlegel, H. B. Reaction Path Following in Mass-Weighted Internal Coordinates. *J. Phys. Chem.* **1990**, *94*, 5523−5527.

(25) Huber, K. P.; Herzberg, G. *Molecular Spectra and Molecular Structure. IV. Constants of Diatomic Molecules*; Van Nostrand Co.: New York, 1979.

(26) *NIST Computational Chemistry Comparison and Benchmark DataBase*, NIST Standard Reference Database Number 101, Release 16a, August 2013. http://cccbdb.nist.gov/ (accessed January 10, 2014).

(27) Pfaendtner, J.; Yu, X.; Broadbelt, L. J. *Calctherm*, version 0.9; Northwestern University: Evanston, IL, 2005.

(28) Pfaendtner, J.; Yu, X.; Broadbelt, L. J. The 1-D Hindered Rotor Approximation. *Theor. Chem. Acc.* **2007**, *118*, 881−898.

(29) Watts, J. D.; Gauss, J.; Bartlett, R. J. Coupled-Cluster Methods with Noniterative Triple Excitations for Restricted Open-Shell Hartree−Fock and Other General Single Determinant Reference Functions. Energies and Analytical Gradients. *J. Chem. Phys.* **1983**, *98*, 8718−8733.

(30) Urban, M.; Kellö, V. Some Trends in Relativistic and Electron Correlation Effects in Electric Properties of Small Molecules. In *Advances in Quantum Chemistry*; Jensen, H. J. Å., Ed.; Academic Press: Amsterdam, The Netherlands, 2005; Vol. *50*, pp 249−269.

(31) Iliaš, M.; Kellö, V.; Urban, M. Relativistic Effects in Atomic and Molecular Properties. *Acta Phys. Slovaca* **2010**, *60*, 259−391.

(32) Karlström, G.; Lindh, R.; Malmqvist, P.-Å.; Roos, B. O.; Ryde, U.; Veryazov, V.; Widmark, P.-O.; Cossi, M.; Schimmelpfennig, B.; Neogrády, P.; et al. MOLCAS: A Program Package for Computational Chemistry. *Comput. Mater. Sci.* **2003**, *28*, 222−239.

(33) Douglas, N.; Kroll, N. M. Quantum Electrodynamical Corrections to the Fine Structure of Helium. *Ann. Phys.* **1974**, *82*, 89−155.

(34) Hess, B. A. Relativistic Electronic-Structure Calculations Employing a Two-Component No-Pair Formalism with External-Field Projection Operators. *Phys. Rev. A: At., Mol., Opt. Phys.* **1986**, *33*, 3742−3748.

(35) Roos, B. O.; Lindh, R.; Malmqvist, P.-Å.; Veryazov, V.; Widmark, P.-O. Main Group Atoms and Dimers Studied with a New Relativistic ANO Basis Set. *J. Phys. Chem. A* **2005**, *108*, 2851−2858.

(36) Widmark, P.-O.; Malmqvist, P.-Å.; Roos, B. O. Density Matrix Averaged Atomic Natural Orbital (ANO) Basis Sets for Correlated Molecular Wave Functions I. First Row Atoms. *Theor. Chem. Acc.* **1990**, *77*, 291−306.

(37) Neogrády, P.; Urban, M.; Hubač, I. Spin Adapted Restricted Hartree−Fock Reference Coupled Cluster Theory for Open Shell Systems. *J. Chem. Phys.* **1994**, *100*, 3706−3716.
(38) Neogrády, P.; Urban, M. Spin-Adapted Restricted Hartree−Fock Reference Coupled-Cluster Theory for Open-Shell Systems: Noniterative Triples for Noncanonical Orbitals. *Int. J. Quantum Chem.* **1995**, *55*, 187−203.
(39) Goodson, D. Z. Extrapolating the Coupled-Cluster Sequence toward the Full Configuration-Interaction Limit. *J. Chem. Phys.* **2002**, *116*, 6948−6956.
(40) Mečiarová, K.; Cantrel, L.; Černušák, I. Thermodynamic Data of Iodine Reactions Calculated by Quantum Chemistry. Training Set of Molecules. *Collect. Czech. Chem. Commun.* **2008**, *73*, 1340−1356.
(41) Jasper, A. W.; Klippenstein, S. J.; Harding, L. B. The Effect of Spin−Orbit Splitting on the Association Kinetics of Barrierless Halogen Atom−Hydrocarbon Radical Reactions. *J. Phys. Chem. A* **2010**, *114*, 5759−5768.
(42) Mečiarová, K.; Šulka, M.; Canneaux, S.; Louis, F.; Černušák, I. A. Theoretical Study of the Kinetics of the Forward and Reverse Reactions HI + CH_3 = I + CH_4. *Chem. Phys. Lett.* **2011**, *517*, 149−154.
(43) Roos, B. O.; Malmqvist, P. Relativistic Quantum Chemistry: The Multiconfigurational Approach. *Phys. Chem. Chem. Phys.* **2004**, *6*, 2919−2927.
(44) Aquilante, F.; De Vico, L.; Ferré, N.; Ghigo, G.; Malmqvist, P.-Å.; Neogrády, P.; Pedersen, T. B.; Pitoňák, M.; Reiher, M.; Roos, B. O.; et al. MOLCAS 7: The Next Generation. *J. Comput. Chem.* **2010**, *31*, 224−247.
(45) Veryazov, V.; Widmark, P.-O.; Serrano-Andres, L.; Lindh, R.; Roos, B. O. 2MOLCAS as a Development Platform for Quantum Chemistry Software. *Int. J. Quantum Chem.* **2004**, *100*, 626−635.
(46) Hess, B. A.; Buenker, R. J.; Marian, C. M.; Peyerimhoff, S. D. Investigation of Electron Correlation on the Theoretical Prediction of Zero-Field Splittings of $^2\Pi$ Molecular States. *Chem. Phys. Lett.* **1982**, *89*, 459−462.
(47) Chase, M. W. *NIST-JANAF Thermochemical Tables*, 4th ed. *J. Phys. Chem. Ref. Data* **1998**, Monograph No. *9*.
(48) Stevens, J. E.; Cui, Q.; Morokuma, K. An Ab Initio Investigation of Spin-Allowed and Spin-Forbidden Pathways of the Gas Phase Reactions of $O(^3P)$+C_2H_5I. *J. Chem. Phys.* **1998**, *108*, 1544−1551.
(49) Hammond, G. S. A Correlation of Reaction Rates. *J. Am. Chem. Soc.* **1955**, *77*, 334−338.
(50) Eyring, H. The Activated Complex in Chemical Reactions. *J. Chem. Phys.* **1935**, *3*, 107−115.
(51) Johnston, H. S. *Gas Phase Reaction Rate Theory*; The Roland Press Co.: New York, 1966.
(52) Laidler, K. J. *Theories of Chemical Reaction Rates*; McGraw-Hill: New York, 1969.
(53) Weston, R. E.; Schwartz, H. A. *Chemical Kinetics*; Prentice-Hall: New York, 1972.
(54) Rapp, D. *Statistical Mechanics*; Holt, Reinhard, and Winston: New York, 1972.
(55) Nikitin, E. E. *Theory of Elementary Atomic and Molecular Processes in Gases*; Claredon Press: Oxford, U.K., 1974.
(56) Smith, I. W. *Kinetics and Dynamics of Elementary Gas Reactions*; Butterworths: London, 1980.
(57) Steinfeld, J. I.; Francisco, J. S.; Hase, W. L. *Chemical Kinetics and Dynamics*; Prentice-Hall: Englewood Cliffs, NJ, 1989.
(58) Eckart, C. The Penetration of a Potential Barrier by Electrons. *Phys. Rev.* **1930**, *35*, 1303−1309.
(59) Garrett, B. C.; Truhlar, D. G. Semiclassical Tunneling Calculations. *J. Phys. Chem.* **1979**, *83*, 2921−2926.
(60) Garrett, B. C.; Truhlar, D. G.; Grev, R. S.; Magnuson, A. W. Improved Treatment of Threshold Contributions in Variational Transition-State Theory. *J. Phys. Chem.* **1980**, *84*, 1730−1748.
(61) Skodje, R. T.; Truhlar, D. G.; Garrett, B. C. A General Small-Curvature Approximation for Transition-State-Theory Transmission Coefficients. *J. Phys. Chem.* **1981**, *85*, 3019−3023.
(62) Skodje, R. T.; Truhlar, D. G.; Garrett, B. C. Vibrationally Adiabatic Models for Reactive Tunneling. *J. Chem. Phys.* **1982**, *77*, 5955−5976.
(63) Truhlar, D.; Issacson, A.; Skodje, R.; Garrett, B. Additions and Corrections - Incorporation of Quantum Effects in Generalized-Transition-State Theory. *J. Phys. Chem.* **1983**, *87*, 4554−4554.
(64) Garrett, B. C.; Truhlar, D. G. WKB Approximation for the Reaction-Path Hamiltonian: Application to Variational Transition State Theory, Vibrationally Adiabatic Excited-State Barrier Heights, and Resonance Calculations. *J. Chem. Phys.* **1984**, *81*, 309−317.
(65) Truhlar, D. G.; Garrett, B. C. Variational Transition State Theory. *Annu. Rev. Phys. Chem.* **1984**, *35*, 159−189.
(66) Miller, W. H.; Smith, F. T. Semiclassical Perturbation Theory of Electron−Molecule Collisions. *Phys. Rev. A: At., Mol., Opt. Phys.* **1978**, *17*, 939−953.
(67) Miller, W. H.; Shi, S. Unified Semiclassical Perturbation and Infinite Order Sudden Approximation, with Application to the Reaction Path Hamiltonian Model. *J. Chem. Phys.* **1981**, *75*, 2258−2264.
(68) Miyoshi, A. *GPOP software*, rev. 2013.07.15m4. http://www.frad.t.u-tokyo.ac.jp/~miyoshi/gpop/ (2014).
(69) Rayez, M.-T.; Rayez, J.-C.; Sawerysyn, J.-P. Ab Initio Studies of the Reactions of Chlorine Atoms with Fluoro- and Chloro-Substituted Methanes. *J. Phys. Chem.* **1994**, *98*, 11342−11352.
(70) Kudchadker, S. A.; Kudchadker, A. P. Ideal Gas Thermodynamic Properties of the Eight Bromo- and Iodomethanes. *J. Phys. Chem. Ref. Data* **1975**, *4*, 457−470.
(71) Kudchadker, S. A.; Kudchadker, A. P. Erratum: Ideal Gas Thermodynamic Properties of Eight Bromo- and Iodomethanes. *J. Phys. Chem. Ref. Data* **1976**, *5*, 529−530.
(72) Carson, A. S.; Laye, P. G.; Pedley, J. B.; Welsby, A. M. The Enthalpies of Formation of Iodomethane, Diiodomethane, Triiodomethane, and Tetraiodomethane by Rotating Combustion Calorimetry. *J. Chem. Thermodyn.* **1993**, *25*, 261−269.
(73) Seetula, J. A. Kinetics of the R + HBr → RH + Br (R = CH_2I or CH_3) Reaction. An Ab Initio Study of the Enthalpy of Formation of the CH_2I, CHI_2 and CI_3 Radicals. *Phys. Chem. Chem. Phys.* **2002**, *4*, 455−460.
(74) Šulková, K.; Federič, J.; Louis, F.; Cantrel, L.; Demovič, L.; Černušák, I. Thermochemistry of Small Iodine Species. *Phys. Scr.* **2013**, *88*, 058304.
(75) Prather, M.; Spivakovsky, C. M. Tropospheric OH and the Lifetimes of Hydrochlorofluorocarbons. *J. Geophys. Res.: Atmos.* **1990**, *95*, 18723−18729.
(76) Louis, F.; Gonzalez, C. A.; Huie, R. E.; Kurylo, M. J. An Ab Initio Study of the Kinetics of the Reactions of Halomethanes with the Hydroxyl Radical. 3. Kinetic Parameters Predictions for the Potential Halon Replacements CH_2FBr, $CHFBr_2$, CHFClBr, $CHCl_2Br$, and $CHClBr_2$. *J. Phys. Chem. A* **2000**, *105*, 1599−1604.
(77) McMillen, D. F.; Golden, D. M. Hydrocarbon Bond Dissociation Energies. *Annu. Rev. Phys. Chem.* **1982**, *33*, 493−532.
(78) Brown, A. C.; Canosa-Mas, C. E.; Wayne, R. P. A Kinetic Study of the Reactions of OH with CH_3I and CF_3I. *Atmos. Environ., Part A* **1990**, *24*, 361−367.
(79) Gilles, M. K.; Turnipseed, A. A.; Talukdar, R. K.; Rudich, Y.; Villalta, P. W.; Huey, L. G.; Burkholder, J. B.; Ravishankara, A. R. Reactions of $O(^3P)$ with Alkyl Iodides: Rate Coefficients and Reaction Products. *J. Phys. Chem.* **1996**, *100*, 14005−14015.
(80) Cotter, E. S. N.; Canosa-Mas, C. E.; Manners, C. R.; Wayne, R. P.; Shallcross, D. E. Kinetic Study of the Reactions of OH with the Simple Alkyl Iodides: CH_3I, C_2H_5I, 1-C_3H_7I and 2-C_3H_7I. *Atmos. Environ.* **2003**, *37*, 1125−1133.
(81) Zhang, S.; Strekowski, R. S.; Bosland, L.; Monod, A.; Zetzsch, C. Kinetic Study of the Reaction of OH with CH_3I Revisited. *Int. J. Chem. Kinet.* **2011**, *43*, 547−556.